Fluid Dynamics — Numerical Techniques

MATH5453M Numerical Exercises 2, 2024

Aly Ilyas
mmai@leeds.ac.uk

Due date: Friday November 15th

Task 1

We begin with the linearized shallow-water system of equations:

$$\frac{\partial \eta}{\partial t} + \frac{\partial (Hu)}{\partial x} = 0, \frac{\partial u}{\partial t} + \frac{\partial (g\eta)}{\partial x} = 0, \tag{1}$$

where we let $u = u(x,t)$ be the velocity, $\eta = \eta(x,t)$ be the free-surface deviation, H_0 be the constant rest depth, and g be the gravitational acceleration.

The variables are scaled as follows:

$$u = U_0 u', \quad x = L_s x', \quad t = \frac{L_s}{U_0} t', \quad \eta = H_{0s} \eta', \quad H = H_{0s} H',$$

where U_0 is a reference velocity, L_s is a characteristic length, and H_{0s} is a characteristic water depth. The dimensionless gravity g' is given by:

$$g' = \frac{g H_{0s}}{U_0^2}.$$

Now, we are substituting the scaled variables into the equations (1), for first equation:

$$\frac{\partial \eta}{\partial t} + \frac{\partial (Hu)}{\partial x} = 0, \tag{2}$$

the time derivative of η becomes:

$$\frac{\partial \eta}{\partial t} = \frac{U_0}{L_s} H_{0s} \frac{\partial \eta'}{\partial t'},$$

and the spatial derivative of Hu becomes:

$$\frac{\partial(Hu)}{\partial x} = H_{0s}U_0 \left(\frac{\partial H'u'}{\partial x'}\right) \frac{1}{L_s}.$$

Thus the first equation (2) becomes:

$$\frac{H_{0s}U_0}{L_s} \left(\frac{\partial \eta'}{\partial t'} + \frac{\partial H'u'}{\partial x'}\right) = 0. \tag{3}$$

For second equation of (1):

$$\frac{\partial u}{\partial t} + \frac{\partial(g\eta)}{\partial x} = 0, \tag{4}$$

The time derivative of u becomes:

$$\frac{\partial u}{\partial t} = \frac{U_0^2}{L_s}\frac{\partial u'}{\partial t'},$$

and the spatial derivative of $g\eta$ becomes:

$$\frac{\partial(g\eta)}{\partial x} = \frac{g'U_0^2 H_{0s}}{L_s}\frac{\partial \eta'}{\partial x'}.$$

Thus, the second equation (4) becomes:

$$\frac{U_0^2}{L_s} \left(\frac{\partial u'}{\partial t'} + g'\frac{\partial \eta'}{\partial x'}\right) = 0. \tag{5}$$

And finally, we got the scaled (dimensionless) form of the shallow-water equations as:

$$\frac{\partial \eta'}{\partial t'} + \frac{\partial H'u'}{\partial x'} = 0, \tag{6}$$

and

$$\frac{\partial u'}{\partial t'} + g'\frac{\partial \eta'}{\partial x'} = 0. \tag{7}$$

As we can see clearly, the scaled form look the same as the original equation (1). Therefore from this point we drop the primes.

Now for a special case where $H(x) = H_o$ constant, we are given the scaled, linearized shallow-water equations:

$$\frac{\partial \eta}{\partial t} + \frac{\partial(H_0 u)}{\partial x} = 0, \quad \frac{\partial u}{\partial t} + \frac{\partial(g\eta)}{\partial x} = 0. \tag{8}$$

It will be easier to rewrite the equation (8) in the vector form as:

$$\frac{\partial}{\partial t}\begin{pmatrix}\eta\\ u\end{pmatrix}+\frac{\partial}{\partial x}\begin{pmatrix}H_0u\\ g\eta\end{pmatrix}=0. \tag{9}$$

Then, we multiply the second equation from (8) by H_0 so we get:

$$\frac{\partial}{\partial t}\begin{pmatrix}\eta\\ H_0u\end{pmatrix}+\frac{\partial}{\partial x}\begin{pmatrix}H_0u\\ H_0g\eta\end{pmatrix}=0. \tag{10}$$

Since our goal is in this form:

$$\frac{\partial}{\partial t}\begin{pmatrix}\eta\\ H_0u\end{pmatrix}+A\frac{\partial}{\partial x}\begin{pmatrix}\eta\\ H_0u\end{pmatrix}=0, \tag{11}$$

where A is a 2×2 matrix that, when multiplied by $\begin{pmatrix}\eta\\ H_0u\end{pmatrix}$, produces the vector $\begin{pmatrix}H_0u\\ H_0g\eta\end{pmatrix}$.

To find A, we set up the matrix equation:

$$A\begin{pmatrix}\eta\\ H_0u\end{pmatrix}=\begin{pmatrix}H_0u\\ H_0g\eta\end{pmatrix}.$$

Let's assume:

$$A=\begin{pmatrix}a_{11}&a_{12}\\ a_{21}&a_{22}\end{pmatrix}.$$

Then:

$$A\begin{pmatrix}\eta\\ H_0u\end{pmatrix}=\begin{pmatrix}a_{11}\eta+a_{12}H_0u\\ a_{21}\eta+a_{22}H_0u\end{pmatrix}.$$

For the first component, we want $a_{11}\eta+a_{12}H_0u=H_0u$. This implies:

$$a_{11}=0 \quad \text{and} \quad a_{12}=1.$$

For the second component, we want $a_{21}\eta+a_{22}H_0u=H_0g\eta$. This implies:

$$a_{21}=H_0g \quad \text{and} \quad a_{22}=0.$$

Thus, we have:

$$A=\begin{pmatrix}0&1\\ H_0g&0\end{pmatrix}.$$

Finally, we can rewrite the original equation as:

$$\frac{\partial}{\partial t}\begin{pmatrix}\eta\\ H_0u\end{pmatrix}+A\frac{\partial}{\partial x}\begin{pmatrix}\eta\\ H_0u\end{pmatrix}=0, \tag{12}$$

where

$$A = \begin{pmatrix} 0 & 1 \\ H_0 g & 0 \end{pmatrix},$$

or we can write A as:

$$A = \begin{pmatrix} 0 & 1 \\ c_0^2 & 0 \end{pmatrix}, \tag{13}$$

with $c_0 = \sqrt{H_0 g}$, the wave speed.

To find the eigenvalues of A, we solve the characteristic equation:

$$\det(A - \lambda I) = 0. \tag{14}$$

Substituting $A - \lambda I = \begin{pmatrix} -\lambda & 1 \\ c_0^2 & -\lambda \end{pmatrix}$, we have

$$\det(A - \lambda I) = \lambda^2 - c_0^2 = 0. \tag{15}$$

Thus, the eigenvalues are:

$$\lambda_1 = c_0, \quad \lambda_2 = -c_0. \tag{16}$$

Now, we calculate the eigenvectors associated with $\lambda_1 = c_0$ and $\lambda_2 = -c_0$. For $\lambda_1 = c_0$, we solve:

$$\begin{pmatrix} 0 & 1 \\ c_0^2 & 0 \end{pmatrix} \begin{pmatrix} 1 \\ c_0 \end{pmatrix} = c_0 \begin{pmatrix} 1 \\ c_0 \end{pmatrix}. \tag{17}$$

For $\lambda_2 = -c_0$, we solve:

$$\begin{pmatrix} 0 & 1 \\ c_0^2 & 0 \end{pmatrix} \begin{pmatrix} 1 \\ -c_0 \end{pmatrix} = -c_0 \begin{pmatrix} 1 \\ -c_0 \end{pmatrix}. \tag{18}$$

Thus, The eigenvector for λ_1 is $\begin{pmatrix} 1 \\ c_0 \end{pmatrix}$ and the eigenvector for λ_2 is $\begin{pmatrix} 1 \\ -c_0 \end{pmatrix}$.

Then we construct the matrix B of eigenvectors:

$$B = \begin{pmatrix} 1 & 1 \\ c_0 & -c_0 \end{pmatrix}. \tag{19}$$

To make B normalized or simplify calculations in later steps, we apply a scaling factor of $\frac{1}{2c_0}$. This gives:

$$B = \frac{1}{2c_0} \begin{pmatrix} 1 & -1 \\ c_0 & c_0 \end{pmatrix}. \tag{20}$$

The scaling factor doesn't change the eigenvalues or the directions of the eigenvectors, but it helps make B and its inverse B^{-1} easier to work with. The inverse of B will now have a simpler form, which can simplify calculations when we later compute $B^{-1}AB$.

Now we look for B^{-1}, note that the determinan of a 2×2 matrix $\begin{pmatrix} a & b \\ c & d \end{pmatrix}$ is given by:

$$\det(B) = ad - bc. \tag{21}$$

For our matrix B (20), we have:

$$a = \frac{1}{2c_0}, \quad b = \frac{-1}{2c_0}, \quad c = \frac{c_0}{2c_0} = \frac{1}{2}, \quad d = \frac{c_0}{2c_0} = \frac{1}{2}.$$

Thus, the determinant of B is:

$$\det(B) = \left(\frac{1}{2c_0}\right) \cdot \left(\frac{1}{2}\right) - \left(\frac{-1}{2c_0}\right) \cdot \left(\frac{1}{2}\right),$$

$$\det(B) = \frac{1}{4c_0} + \frac{1}{4c_0} = \frac{2}{4c_0} = \frac{1}{2c_0}.$$

So the inverse of B is:

$$B^{-1} = \frac{1}{\frac{1}{2c_0}} \begin{pmatrix} \frac{1}{2} & \frac{1}{2c_0} \\ -\frac{1}{2} & \frac{1}{2c_0} \end{pmatrix},$$

$$B^{-1} = 2c_0 \begin{pmatrix} \frac{1}{2} & \frac{1}{2c_0} \\ -\frac{1}{2} & \frac{1}{2c_0} \end{pmatrix},$$

$$B^{-1} = \begin{pmatrix} c_0 & 1 \\ -c_0 & 1 \end{pmatrix}. \tag{22}$$

We already have (13), (20), and (22). To diagonalize A, we compute:

$$\begin{aligned} B^{-1}AB &= \begin{pmatrix} c_0 & 1 \\ -c_0 & 1 \end{pmatrix} \begin{pmatrix} 0 & 1 \\ c_0^2 & 0 \end{pmatrix} \left[\frac{1}{2c_0} \begin{pmatrix} 1 & -1 \\ c_0 & c_0 \end{pmatrix}\right], \\ &= \begin{pmatrix} c_0 & 1 \\ -c_0 & 1 \end{pmatrix} \begin{pmatrix} 0 & 1 \\ c_0^2 & 0 \end{pmatrix} \begin{pmatrix} \frac{1}{2c_0} & \frac{-1}{2c_0} \\ \frac{1}{2} & \frac{1}{2} \end{pmatrix}, \\ &= \begin{pmatrix} c_0^2 & c_0^2 \\ c_0 & -c_0 \end{pmatrix} \begin{pmatrix} \frac{1}{2c_0} & \frac{-1}{2c_0} \\ \frac{1}{2} & \frac{1}{2} \end{pmatrix}, \\ &= \begin{pmatrix} c_0 & 0 \\ 0 & -c_0 \end{pmatrix}. \end{aligned} \tag{23}$$

Now, we define the Riemann invariants r_1 and r_2:

$$r = (r_1, r_2)^T = B^{-1} \begin{pmatrix} \eta \\ H_0 u \end{pmatrix}. \tag{24}$$

The definiton (24) gives us:

$$\begin{pmatrix} r_1 \\ r_2 \end{pmatrix} = \begin{pmatrix} c_0 & 1 \\ -c_0 & 1 \end{pmatrix} \begin{pmatrix} \eta \\ H_0 u \end{pmatrix}. \tag{25}$$

Therefore we get:

$$r_1 = H_0 u + c_0 \eta, \quad r_2 = H_0 u - c_0 \eta. \tag{26}$$

To show that the system can be rewritten as a decoupled set of linear advection equations, we proceed as follows.

First we already have matrix form of (13) and (22), then we rewrite the system using (24). We let $\begin{pmatrix} \eta \\ H_0 u \end{pmatrix} = Br$, where $r = \begin{pmatrix} r_1 \\ r_2 \end{pmatrix}$, so we have:

$$\begin{pmatrix} \eta \\ H_0 u \end{pmatrix} = B \begin{pmatrix} r_1 \\ r_2 \end{pmatrix}. \tag{27}$$

Next we differentiate with respect to t. Taking the time derivative of both sides, we get:

$$\frac{\partial}{\partial t} \begin{pmatrix} \eta \\ H_0 u \end{pmatrix} = B \frac{\partial r}{\partial t}. \tag{28}$$

Then, we substitute (28) into the original equation (12) and we get:

$$B \frac{\partial r}{\partial t} + AB \frac{\partial r}{\partial x} = 0. \tag{29}$$

Multiplying both sides by B^{-1} and we get:

$$\frac{\partial r}{\partial t} + B^{-1} AB \frac{\partial r}{\partial x} = 0. \tag{30}$$

Now, we subtitute $B^{-1}AB$ from (23) and we get the equation in decoupled form as:

$$\frac{\partial r}{\partial t} + \begin{pmatrix} \lambda_1 & 0 \\ 0 & \lambda_2 \end{pmatrix} \frac{\partial r}{\partial x} = 0. \tag{31}$$

This is a decoupled set of linear advection equations for r_1 and r_2, with advection speeds $\lambda_1 = c_0$ and $\lambda_2 = -c_0$.

Task 1: additional

Recall that we are given the scaled, linearized shallow-water equations (8), now we will let the first equation be the continuity equation as:

$$\frac{\partial \eta}{\partial t} + \frac{\partial H_0 u}{\partial x} = 0, \tag{32}$$

and the second equation be the momentum equation as:

$$\frac{\partial u}{\partial t} + \frac{\partial g\eta}{\partial x} = 0. \tag{33}$$

We then multiply the continuity equation (32) by $c_0 = \sqrt{gH_0}$:

$$c_0\frac{\partial \eta}{\partial t} + c_0\frac{\partial H_0 u}{\partial x} = 0, \tag{34}$$

and multiply the momentum equation (33) by H_0:

$$H_0\frac{\partial u}{\partial t} + H_0\frac{\partial g\eta}{\partial x} = 0. \tag{35}$$

Adding (34) to the momentum equation (35) gives:

$$\left(c_0\frac{\partial \eta}{\partial t} + c_0\frac{\partial H_0 u}{\partial x}\right) + \left(H_0\frac{\partial u}{\partial t} + H_0\frac{\partial g\eta}{\partial x}\right) = 0, \tag{36}$$

Rearrange (36) be:

$$\left(H_0\frac{\partial u}{\partial t} + c_0\frac{\partial \eta}{\partial t}\right) + \left(c_0\frac{\partial H_0 u}{\partial x} + H_0\frac{\partial g\eta}{\partial x}\right) = 0,$$

$$\left(\frac{\partial H_0 u}{\partial t} + \frac{\partial c_0\eta}{\partial t}\right) + \left(c_0\frac{\partial H_0 u}{\partial x} + H_0 g\frac{\partial \eta}{\partial x}\right) = 0.$$

Recall that $c_0 = \sqrt{gH_0}$ so we get:

$$\left(\frac{\partial H_0 u}{\partial t} + \frac{\partial c_0\eta}{\partial t}\right) + \left(c_0\frac{\partial H_0 u}{\partial x} + {c_0}^2\frac{\partial \eta}{\partial x}\right) = 0.$$

$$\left(\frac{\partial H_0 u}{\partial t} + \frac{\partial c_0\eta}{\partial t}\right) + c_0\left(\frac{\partial H_0 u}{\partial x} + \frac{\partial c_0\eta}{\partial x}\right) = 0.$$

Finally we got the form of equation (31) as :

$$\frac{\partial}{\partial t}\left(H_0 u + c_0\eta\right) + c_0\frac{\partial}{\partial x}\left(H_0 u + c_0\eta\right) = 0, \tag{37}$$

that define the first Riemann invariant:

$$r_1 = H_0 u + c_0 \eta. \tag{38}$$

For the second Riemann invariant, we recall the equation (32) and (33), we then multiply the continuity equation (32) by $-c_0$ and get:

$$-c_0 \frac{\partial \eta}{\partial t} - c_0 \frac{\partial H_0 u}{\partial x} = 0, \tag{39}$$

and multiply the momentum equation (33) by H_0:

$$H_0 \frac{\partial u}{\partial t} + H_0 \frac{\partial g\eta}{\partial x} = 0. \tag{40}$$

Adding (39) to the equation (40) gives:

$$\left(-c_0 \frac{\partial \eta}{\partial t} - c_0 \frac{\partial H_0 u}{\partial x}\right) + \left(H_0 \frac{\partial u}{\partial t} + H_0 \frac{\partial g\eta}{\partial x}\right) = 0, \tag{41}$$

Rearrange (41) be:

$$\left(H_0 \frac{\partial u}{\partial t} - c_0 \frac{\partial \eta}{\partial t}\right) + \left(-c_0 \frac{\partial H_0 u}{\partial x} + H_0 \frac{\partial g\eta}{\partial x}\right) = 0,$$

$$\left(\frac{\partial H_0 u}{\partial t} - \frac{\partial c_0 \eta}{\partial t}\right) + \left(-c_0 \frac{\partial H_0 u}{\partial x} + H_0 g \frac{\partial \eta}{\partial x}\right) = 0.$$

Recall that $c_0 = \sqrt{gH_0}$ so we get:

$$\left(\frac{\partial H_0 u}{\partial t} - \frac{\partial c_0 \eta}{\partial t}\right) + \left(-c_0 \frac{\partial H_0 u}{\partial x} + {c_0}^2 \frac{\partial \eta}{\partial x}\right) = 0.$$

Factoring out $-c_0$ on second term and we get:

$$\left(\frac{\partial H_0 u}{\partial t} - \frac{\partial c_0 \eta}{\partial t}\right) - c_0 \left(\frac{\partial H_0 u}{\partial x} - \frac{\partial c_0 \eta}{\partial x}\right) = 0.$$

Thus, we got the form of equation (31) as :

$$\frac{\partial}{\partial t}\left(H_0 u - c_0 \eta\right) - c_0 \frac{\partial}{\partial x}\left(H_0 u - c_0 \eta\right) = 0, \tag{42}$$

that define the second Riemann invariant as:

$$r_2 = H_0 u - c_0 \eta. \tag{43}$$

Task 2

We already got the updated system (31), where the matrix of eigenvalues

$$\begin{pmatrix} \lambda_1 & 0 \\ 0 & \lambda_2 \end{pmatrix}$$

represents two independent characteristics for the system, with $\lambda_1 = c_0$ and $\lambda_2 = -c_0$. We also have the piecewise constant initial data for r_1 and r_2:

$$r_1(x,0) = \begin{cases} r_{1l} & \text{for } x < 0, \\ r_{1r} & \text{for } x \geq 0, \end{cases} \quad r_2(x,0) = \begin{cases} r_{2l} & \text{for } x < 0, \\ r_{2r} & \text{for } x \geq 0. \end{cases} \tag{44}$$

This setup describes a typical Riemann problem where there is a discontinuity at $x = 0$ for both r_1 and r_2, and our task is to determine the solution $r(x,t)$ at later times. To solve this system, we use the method of characteristics. Since the system is diagonal, we treat each component independently.

From (37), the equation for r_1 becomes:

$$\frac{\partial r_1}{\partial t} + c_0 \frac{\partial r_1}{\partial x} = 0, \tag{45}$$

and from (42) the equation for r_2 becomes:

$$\frac{\partial r_2}{\partial t} - c_0 \frac{\partial r_2}{\partial x} = 0. \tag{46}$$

These are standard linear advection equations with the respective speeds of propagation.

We solve these equations along the characteristic curves. For r_1, the characteristic curves are given by:

$$x = c_0 t + x_0, \tag{47}$$

where x_0 is the initial position. The solution for r_1 remains constant along these characteristics, so:

$$r_1(x,t) = \begin{cases} r_{1l} & \text{for } x < c_0 t, \\ r_{1r} & \text{for } x \geq c_0 t. \end{cases} \tag{48}$$

Similarly, for r_2, the characteristics are:

$$x = -c_0 t + x_0, \tag{49}$$

and the solution remains constant along these lines. Hence,

$$r_2(x,t) = \begin{cases} r_{2l} & \text{for } x < -c_0 t, \\ r_{2r} & \text{for } x \geq -c_0 t. \end{cases} \tag{50}$$

Next, we express the solutions in terms of the physical variables u and η. The Riemann invariants r_1 and r_2 are related to these physical variables by the equation (17). We can solve for u and η from these equations:

$$H_0 u = \frac{1}{2}(r_1 + r_2), \tag{51}$$

$$\eta = \frac{1}{2c_0}(r_1 - r_2). \tag{52}$$

Thus, to find the solution for $H_0 u(x,t)$ and $\eta(x,t)$, we substitute the solutions for $r_1(x,t)$ and $r_2(x,t)$ into these formulas.

For $x < -c_0 t$, both r_1 and r_2 are equal to their initial values on the left. Therefore,

$$H_0 u(x,t) = H_0 u_l, \quad \eta(x,t) = \eta_l, \tag{53}$$

where

$$H_0 u_l = \frac{1}{2}(r_{1l} + r_{2l}), \quad \eta_l = \frac{1}{2c_0}(r_{1l} - r_{2l}).$$

For $-c_0 t \leq x \leq c_0 t$, in this region, r_1 and r_2 are given by r_{1l} and r_{2r}, respectively. Thus, the solution is constant:

$$H_0 u(x,t) = \frac{1}{2}(r_{1l} + r_{2r}), \quad \eta(x,t) = \frac{1}{2c_0}(r_{1l} - r_{2r}). \tag{54}$$

For $x > c_0 t$, both r_1 and r_2 are equal to their initial values on the right. Hence,

$$H_0 u(x,t) = H_0 u_r, \quad \eta(x,t) = \eta_r, \tag{55}$$

where

$$H_0 u_r = \frac{1}{2}(r_{1r} + r_{2r}), \quad \eta_r = \frac{1}{2c_0}(r_{1r} - r_{2r}).$$

Thus, we can write the final solution for $H_0 u(x,t)$ and $\eta(x,t)$ as:

$$H_0 u(x,t) = \frac{1}{2}(r_1(x,t) + r_2(x,t)) = \begin{cases} H_0 u_l & \text{for } x < -c_0 t, \\ \frac{1}{2}(r_{1l} + r_{2r}) & \text{for } -c_0 t \leq x \leq c_0 t, \\ H_0 u_r & \text{for } x > c_0 t, \end{cases} \tag{56}$$

$$\eta(x,t) = \frac{1}{2c_0}(r_1(x,t) - r_2(x,t)) = \begin{cases} \eta_l & \text{for } x < -c_0 t, \\ \frac{1}{2c_0}(r_{1l} - r_{2r}) & \text{for } -c_0 t \le x \le c_0 t, \\ \eta_r & \text{for } x > c_0 t. \end{cases} \tag{57}$$

If we define the Riemann invariants as:

$$r_1 = H_0 u + \sqrt{gH_0}\,\eta, \quad r_2 = H_0 u - \sqrt{gH_0}\,\eta,$$

then we can write the final solutions for $H_0 u(x,t)$ and $\eta(x,t)$ as:

$$H_0 u(x,t) = \begin{cases} H_0 u_l & \text{for } x < -c_0 t, \\ \frac{1}{2}\left(H_0 u_l + \sqrt{gH_0}\,\eta_l + H_0 u_r - \sqrt{gH_0}\,\eta_r\right) & \text{for } -c_0 t \le x \le c_0 t, \\ H_0 u_r & \text{for } x > c_0 t, \end{cases} \tag{58}$$

$$\eta(x,t) = \begin{cases} \eta_l & \text{for } x < -c_0 t, \\ \frac{1}{2\sqrt{gH_0}}\left(H_0 u_l + \sqrt{gH_0}\,\eta_l - H_0 u_r + \sqrt{gH_0}\,\eta_r\right) & \text{for } -c_0 t \le x \le c_0 t, \\ \eta_r & \text{for } x > c_0 t. \end{cases} \tag{59}$$

If we simplify the final solution further, then we get:

$$H_0 u(x,t) = \begin{cases} H_0 u_l & \text{for } x < -c_0 t, \\ \frac{1}{2}\left(H_0(u_l + u_r) + \sqrt{gH_0}(\eta_l - \eta_r)\right) & \text{for } -c_0 t \le x \le c_0 t, \\ H_0 u_r & \text{for } x > c_0 t, \end{cases} \tag{60}$$

$$\eta(x,t) = \begin{cases} \eta_l & \text{for } x < -c_0 t, \\ \frac{1}{2\sqrt{gH_0}}\left(H_0(u_l - u_r) + \sqrt{gH_0}(\eta_l - \eta_r)\right) & \text{for } -c_0 t \le x \le c_0 t, \\ \eta_r & \text{for } x > c_0 t. \end{cases} \tag{61}$$

Therefore, the solution demonstrates that $H_0 u(x,t)$ and $\eta(x,t)$ are piecewise continuous, consisting of three distinct regions. The values remain constant in the regions $x < -c_0 t$ and $x > c_0 t$, corresponding to the initial left and right states. In the intermediate region $-c_0 t \le x \le c_0 t$, the solution is determined by a combination of the Riemann invariants from the left and right states, leading to a transition zone between $H_0 u_l, \eta_l$ and $H_0 u_r, \eta_r$. This structure reflects the propagation of characteristics with speeds $\pm c_0$, as expected for the given hyperbolic system.

Task 3

To apply the Godunov scheme to the system of equations (8) and derive a time step estimate, we need to follow the steps of the Godunov method, which is based on solving the Riemann problem at each grid interface. The solution to the Riemann problem provides the numerical fluxes, which are then used to update the variables at each grid point.

We are working with the following system of equations:

$$\frac{\partial \eta}{\partial t} + \frac{\partial (H_0 u)}{\partial x} = 0, \quad \frac{\partial u}{\partial t} + \frac{\partial (g\eta)}{\partial x} = 0.$$

The Godunov scheme requires computing the numerical flux at each cell interface. For our system, we define the physical flux for the η-equation as:

$$f_\eta(x,t) = H_0 u, \tag{62}$$

and the physical flux for the u-equation as:

$$f_u(x,t) = g\eta. \tag{63}$$

In Godunov's method, we first discretize both space and time. Denote the grid points as x_i with grid spacing Δx, and the time levels as t^n with time step Δt. Let η_i^n and u_i^n represent the discrete values of $\eta(x_i, t^n)$ and $u(x_i, t^n)$ at the grid point x_i and the time step t^n.

First, we apply a first-order finite difference scheme in time (explicit scheme) and a central difference scheme in space to the governing equations. For the η-equation:

$$\frac{\partial \eta}{\partial t} + \frac{\partial (H_0 u)}{\partial x} = 0,$$

we discretize the time derivative and the spatial derivative:

$$\frac{\eta_i^{n+1} - \eta_i^n}{\Delta t} + \frac{H_0(u_{i+1}^{n+1} - u_{i-1}^{n+1})}{2\Delta x} = 0. \tag{64}$$

This is rearranged to give the update for η_i^{n+1}:

$$\eta_i^{n+1} = \eta_i^n - \frac{\Delta t}{\Delta x}\left(F_\eta^{i+\frac{1}{2}} - F_\eta^{i-\frac{1}{2}}\right), \tag{65}$$

where $F_\eta^{i+\frac{1}{2}}$ and $F_\eta^{i-\frac{1}{2}}$ are the numerical fluxes at the interfaces $i + \frac{1}{2}$ and $i - \frac{1}{2}$, respectively.

Similarly, for the u-equation:

$$\frac{\partial u}{\partial t} + \frac{\partial (g\eta)}{\partial x} = 0,$$

we discretize in time and space:

$$\frac{u_i^{n+1} - u_i^n}{\Delta t} + \frac{g(\eta_{i+1}^{n+1} - \eta_{i-1}^{n+1})}{2\Delta x} = 0. \tag{66}$$

This gives the update for u_i^{n+1}:

$$u_i^{n+1} = u_i^n - \frac{\Delta t}{\Delta x}\left(F_u^{i+\frac{1}{2}} - F_u^{i-\frac{1}{2}}\right), \tag{67}$$

where $F_u^{i+\frac{1}{2}}$ and $F_u^{i-\frac{1}{2}}$ are the numerical fluxes for the velocity at the respective interfaces.

At the interface $x_{i+\frac{1}{2}}$, the numerical fluxes are computed using the left and right states (η_l, u_l) and (η_r, u_r) as follows:

$$F_\eta^{i+\frac{1}{2}} = \frac{1}{2}\left(H_0 u_l + H_0 u_r - |c|(\eta_r - \eta_l)\right), \tag{68}$$

$$F_u^{i+\frac{1}{2}} = \frac{1}{2}\left(g\eta_l + g\eta_r - |c|(u_r - u_l)\right), \tag{69}$$

where c is the wave speed, determined from the system's characteristics.

Similarly, At the interface $x_{i-\frac{1}{2}}$, the numerical fluxes are computed using the left and right states (η_l, u_l) and (η_r, u_r) as follows:

$$F_\eta^{i-\frac{1}{2}} = \frac{1}{2}\left(H_0 u_l + H_0 u_r - |c|(\eta_l - \eta_r)\right), \tag{70}$$

$$F_u^{i-\frac{1}{2}} = \frac{1}{2}\left(g\eta_l + g\eta_r - |c|(u_l - u_r)\right), \tag{71}$$

where c is the wave speed, determined from the system's characteristics. Note that we have speeds c_0 and $-c_0$, so we take $|c| = c_0$, so the equation (68), (69), (70), and (71) become:

$$F_\eta^{i+\frac{1}{2}} = \frac{1}{2}\left(H_0 u_l + H_0 u_r - c_o(\eta_r - \eta_l)\right), \tag{72}$$

$$F_u^{i+\frac{1}{2}} = \frac{1}{2}\left(g\eta_l + g\eta_r - c_o(u_r - u_l)\right), \tag{73}$$

$$F_\eta^{i-\frac{1}{2}} = \frac{1}{2}\left(H_0 u_l + H_0 u_r - c_o(\eta_l - \eta_r)\right), \tag{74}$$

$$F_u^{i-\frac{1}{2}} = \frac{1}{2}\left(g\eta_l + g\eta_r - c_o(u_l - u_r)\right). \tag{75}$$

The stability of the Godunov scheme requires satisfying the CFL condition:

$$\frac{\Delta t}{\Delta x} \leq \frac{1}{|c|}, \tag{76}$$

where $|c|$ is the maximum wave speed in the system.

To estimate $|c|$, we observe that the characteristics for r_1 and r_2 (which are related to η and u) have speeds c_0 and $-c_0$, so we take $|c| = c_0$, and the CFL condition becomes:

$$\frac{\Delta t}{\Delta x} \leq \frac{1}{c_0}. \tag{77}$$

Thus, the time step estimate is:

$$\Delta t \leq \frac{\Delta x}{c_0}. \tag{78}$$

To implement boundary conditions in the Godunov scheme, we use the following methods for an "open" domain and a "closed" domain. For the open domain, we use extrapolating boundary conditions. These conditions allow the solution to propagate freely across the boundary, as if the domain extends indefinitely. For the velocity u at the boundary, the boundary value is set equal to the velocity inside the domain, continued outward:

$$u_{\text{ext}}(x_0, t) = u_{\text{dom}}(x_0, t), \tag{79}$$

where x_0 is the boundary point and u_{dom} is the velocity inside the domain. For the surface elevation η at the boundary, we extrapolate the value using a forward approximation, ensuring that η at the boundary is the same as the last value inside the domain:

$$\eta_{\text{ext}}(x_0, t) = \eta_{\text{dom}}(x_0, t). \tag{80}$$

Thus, in the open domain, both u and η are propagated freely outward.

For a closed domain, we use ghost values to enforce boundary conditions. A ghost cell is a fictitious cell outside the physical domain that is used to enforce boundary conditions. For the velocity u, we enforce that the velocity inside the domain and outside the domain are equal but opposite in sign, which ensures no flux across the boundary:

$$u_{\text{ghost}}(x_0, t) = -u_{\text{dom}}(x_0, t). \tag{81}$$

This reflects a "closed" boundary condition, where the velocity is mirrored across the boundary. For the surface elevation η, we set the ghost value equal to the value inside the domain to maintain continuity across the boundary:

$$\eta_{\text{ghost}}(x_0, t) = \eta_{\text{dom}}(x_0, t). \tag{82}$$

Thus, the boundary is closed, with η being continuous and u mirrored across the boundary.

In the Godunov scheme, the fluxes at the boundary are computed using either the extrapolated values for an open domain or the ghost values for a closed domain.

For the open domain, the boundary fluxes are:

$$f_{\eta,\text{ext}} = H_0 u_{\text{ext}}, \quad f_{u,\text{ext}} = g\eta_{\text{ext}}. \tag{83}$$

For the closed domain, the boundary fluxes are:

$$f_{\eta,\text{ghost}} = H_0 u_{\text{ghost}}, \quad f_{u,\text{ghost}} = g\eta_{\text{ghost}}. \tag{84}$$

These conditions ensure the correct handling of boundaries in the scheme.

For solid wall boundary conditions at $x = 0$ and $x = L$, we enforce no flux through the boundary, meaning the normal flux is set to zero. The velocity u is set to zero at the boundary, reflecting no motion of the fluid at the boundary:

$$u(0,t) = 0 \quad \text{and} \quad u(l,t) = 0. \tag{85}$$

The surface elevation η is continuous at the boundary:

$$\eta(0,t) = \eta_{\text{boundary}} \quad \text{and} \quad \eta(l,t) = \eta_{\text{boundary}}, \tag{86}$$

where η_{boundary} is the value of η at the boundary, either determined based on the solution inside the domain or specified as a boundary condition.

This ensures that no material flows through the boundaries, representing a solid wall where the surface is static, without directly adjusting the flux in the Godunov scheme.

First, consider the case where $H(x)$ is constant. To extend the discretization to handle a continuous but variable $H(x)$, we treat $H(x)$ as being continuous across cell edges. At each computational cell, H_0 is defined as the value of $H(x)$ at the center of the cell, ensuring continuity of $H(x)$ across the domain.

For each cell edge x_i, we use $H_0(x_i)$ as the value of $H(x)$ at the center of the cell. Since $H(x)$ is continuous, the value of H_0 is representative of the true value of $H(x)$ at that point.

At each cell edge, the Riemann solution and flux are computed using the locally constant value of $H(x)$, i.e., $H_0(x_i)$, where $H_0(x_i)$ corresponds to the exact value of $H(x)$ at that cell center. This ensures the continuity of $H(x)$ while allowing the use of the Riemann solver for computing fluxes based on the locally constant approximation of $H(x)$.

Task 4

By using the code in **ex2no4.py** the Godunov scheme was implemented for equation (1). In Figure 1, the Riemann solution was set as the initial condition. The parameters used were $\eta_l = 1$, $\eta_r = 0$, $u_l = 0.5$, and $u_r = 0$, with the initial condition represented by the blue solid line. Figure 1 compares the exact solution (solid lines: orange at time 3, green at time 4) and the numerical solution (marked with 'x', blue at time 3 and orange at time 4) using $CFL = 0.1$. In this case, where there is a discontinuity (a step), the numerical solution transitions smoothly, while the exact solution forms a vertical line, showing a jump at the shock.

In Figure 2, the Godunov scheme was implemented for the same equation and initial conditions as in Figure 1, but with $CFL = 1$. Here, the comparison between the exact solution (solid lines: orange at time 3, green at time 4) and the numerical solution (marked with 'x', blue at time 3 and orange at time 4) shows that the numerical solution closely matches the exact solution, even when a jump in the exact solution (at the shock) is present. This demonstrates the Godunov scheme's ability to accurately capture the shock with a larger CFL value.

When using the Riemann solution as the initial condition, which typically involves a discontinuity such as a shock, the behavior observed with different CFL numbers can be understood in the context of the Godunov scheme. The Godunov scheme is specifically designed to handle such discontinuities effectively. When the CFL number is set to 1, the scheme propagates information through the grid at an optimal rate, allowing the shock to develop and be captured accurately, resulting in a solution that closely matches the exact solution of the Riemann problem.

In contrast, when $CFL = 0.1$, the time step is much smaller relative to the spatial step, causing the solution to evolve more slowly. This slower evolution impedes the propagation of the shock, and numerical diffusion may occur, especially in the smooth regions of the solution. As a result, the shock is not resolved accurately, leading to higher error between the numerical and exact solutions.

The key factor here is the propagation speed of the shock. With $CFL = 1$, the time step is more balanced with the grid resolution, allowing the shock to move at its correct speed. This is crucial for capturing the shock accurately. Smaller CFL numbers, such as $CFL = 0.1$, slow down the propagation, introducing unnecessary numerical dissipation and leading to less accurate results, particularly in the shock region.

Thus, for the Riemann problem, using $CFL = 1$ allows the Godunov scheme to operate near its optimal stability limit, capturing the shock more

accurately and providing a solution that is closer to the exact result. On the other hand, $CFL = 0.1$ introduces excess numerical dissipation, which distorts the shock and increases the error in the numerical solution.

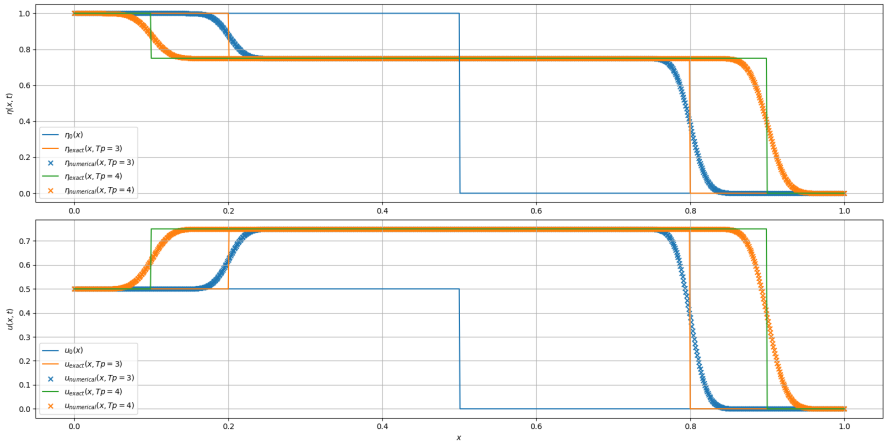

Figure 1: exact and numerical solution comparison for equation (1) using the Riemann solution as the initial condition, with $\eta_l = 1$, $\eta_r = 0$, $u_l = 0.5$, and $u_r = 0$, and using $CFL = 0.1$.

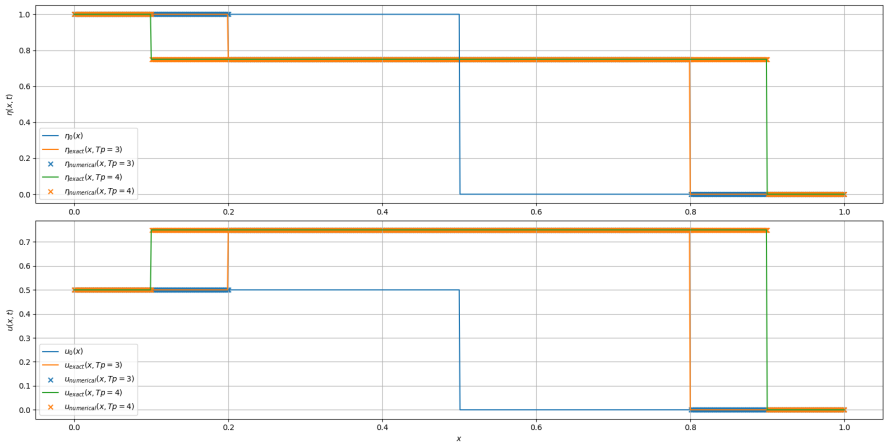

Figure 2: Solution for equation (1) using the Riemann solution as the initial condition, with $\eta_l = 1$, $\eta_r = 0$, $u_l = 0.5$, and $u_r = 0$, and using $CFL = 1$.

For the next case, a standing wave is used with the following initial conditions:

$$u_0(x) = \eta_0(x) = \sin\left(a_m \pi \frac{x}{L_x}\right),$$

where u_0 and η_0 represent the initial velocity and elevation conditions, respectively, and a_m is the mode number. These initial conditions are implemented both in numerical arrays and UFL expressions for comparison. The boundary conditions at x_0 for velocity and elevation are given by:

$$u(x_0) = \eta(x_0) = \sin\left(a_m\pi\frac{x_0}{L_x} - a_m\pi\frac{a}{L_x}(t_0 + \Delta t)\right),$$

where $u(x_0)$ and $\eta(x_0)$ represent the boundary conditions for velocity and elevation, respectively, and a, H_0, t_0, and Δt are constants.

The boundary conditions are then applied as constant values for velocity and elevation at x_0, represented as:

$$u_{\text{in}} = \text{Constant}(u(x_0)), \quad \eta_{\text{in}} = \text{Constant}(\eta(x_0)).$$

Figures 3 and 4 show the numerical solutions for the standing wave problem using $CFL = 0.1$ and $CFL = 1$, respectively. Interestingly, the error is only slightly different between the two cases, with $CFL = 1$ providing a more accurate result. Both cases show that the numerical solution is almost as good as the exact solution.

In both figures, the following representations are used: the blue solid line represents the initial condition, the orange solid line represents the exact solution at time 3, and the blue marker ('-') represents the numerical solution at time 3. The green dashed line represents the error at time 3. Similarly, the red solid line represents the exact solution at time 4, the orange marker ('-') represents the numerical solution at time 4, and the purple dashed line represents the error at time 4. a dashed line is included to represent the error between the exact and numerical solutions, but the magnitude of the error is not emphasized. Even though $CFL = 0.1$ results in slightly higher error, both cases exhibit low error, which can be considered negligible and almost zero. This demonstrates that, for this particular problem, both $CFL = 0.1$ and $CFL = 1$ produce accurate results, with only minimal difference in error, and can be considered reliable for capturing the behavior of the standing wave.

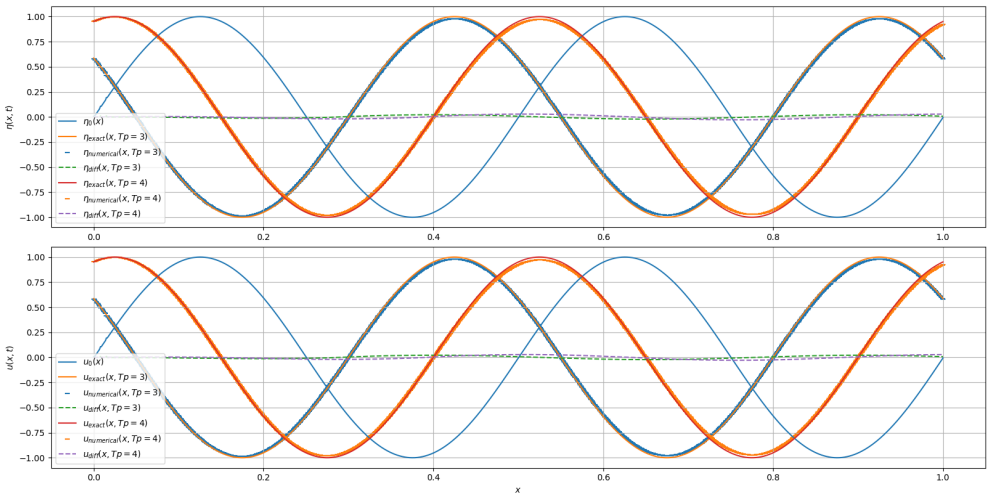

Figure 3: Comparison of numerical and exact solution for equation (1) using the standing wave solution as the initial condition, with $CFL = 0.1$.

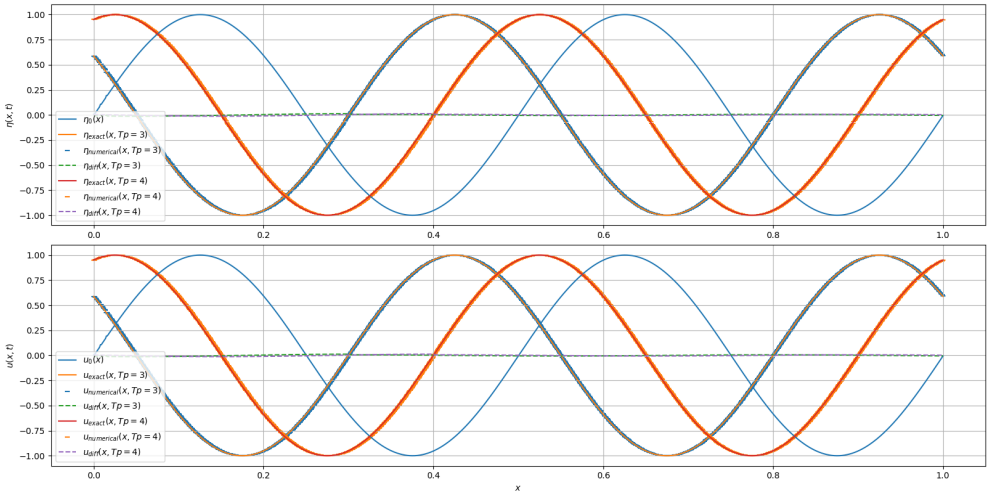

Figure 4: Comparison of numerical and exact solution for equation (1) using the standing wave solution as the initial condition, with $CFL = 1$.

Task 5

We use the given code SWE_DG0.py for this task. In Figure 5, the initial conditions for the standing wave are represented by black markers ('-'), while the exact solution is shown with blue markers ('x'). The numerical solution at a later time is indicated by orange markers ('-'). At time $t = 2$, the numerical solution converges to the exact solution almost perfectly, demonstrating the effectiveness of the numerical method for this problem. The standing wave solution for elevation $\eta(x,t)$ and velocity $u(x,t)$ is defined as:

$$\eta(x,t) = \sin(w_k t)\cos(kx), \quad u(x,t) = -c_0 \cos(w_k t)\sin(kx),$$

where $w_k = kc_0$ is the angular frequency, and $k = \frac{2\pi}{L_x}$ is the wave number. These conditions describe the standing wave with closed boundaries at both ends.

In Figure 6, the energy over time is shown, with the x-axis representing time. The green solid line in Figure 6 represents the energy E_t at each time step, which is computed using the formula:

$$E_t = \frac{1}{2H_0}\int u_2^2\,dx + \frac{1}{2}\int u_1^2\,dx,$$

where $u_1 = H_0 u$ represents the velocity component scaled by the reference height H_0, $u_2 = g\eta$ represents the elevation component scaled by the gravitational acceleration g, H_0 is the reference height and g is the gravitational acceleration.

When observing the difference between the numerical and exact solutions, it is observed that when the energy of the system is high, the difference is also high. This can be explained by several factors. Higher energy often corresponds to larger variations or oscillations in the solution, which are harder to resolve accurately with numerical methods, especially when there are rapid changes in velocity or elevation. These larger variations can introduce greater numerical errors, particularly if the time step or spatial resolution is insufficient to capture the dynamics of the system.

The energy remains relatively stable throughout the simulation, reflecting the conservative nature of the numerical scheme. These results highlight that the numerical solution accurately captures the standing wave behavior, and the scheme performs well in maintaining energy conservation. Even though the numerical solution contains small errors, it converges closely to the exact solution, showcasing the effectiveness of the chosen numerical method.

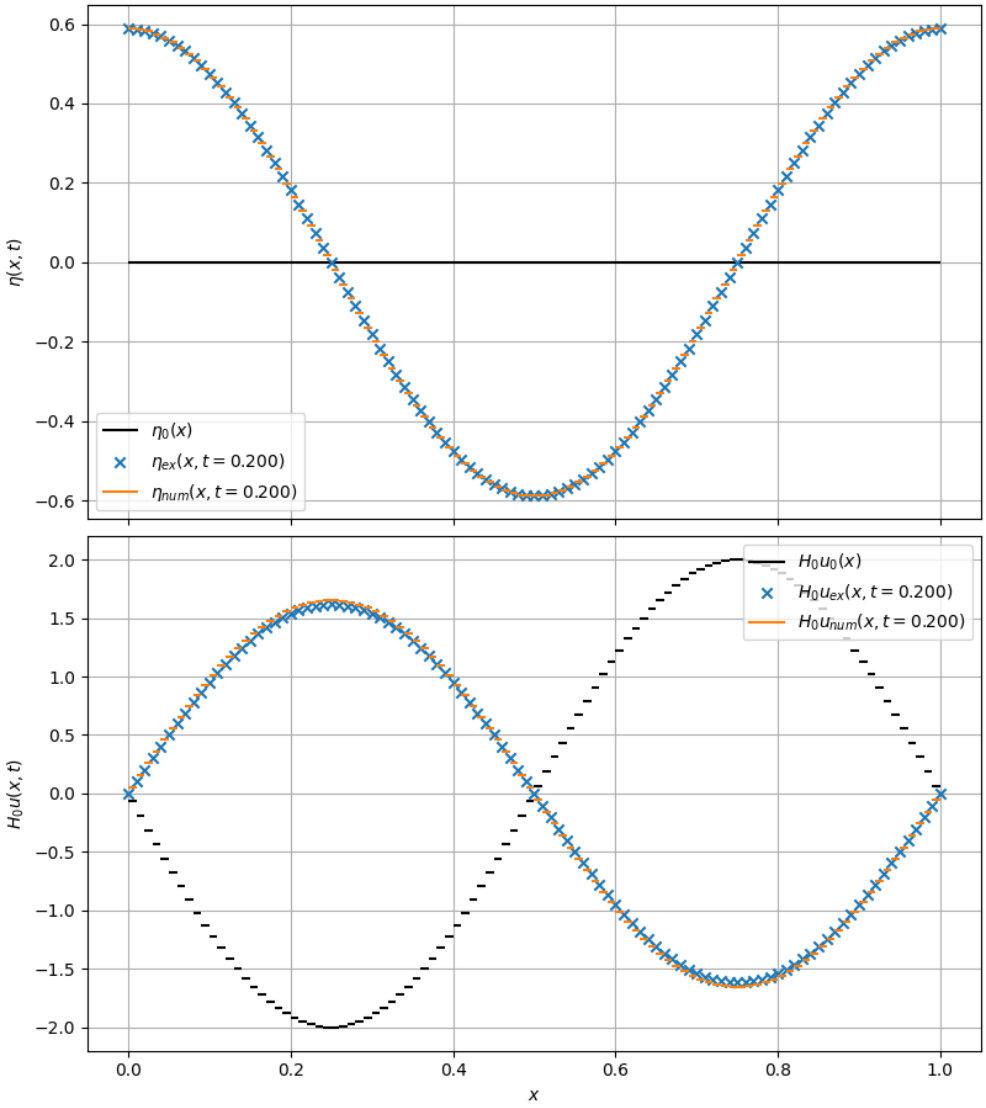

Figure 5: Comparison of numerical and exact solution for equation (1) using the standing wave solution as the initial condition, with alternating flux and $CFL = 1$.

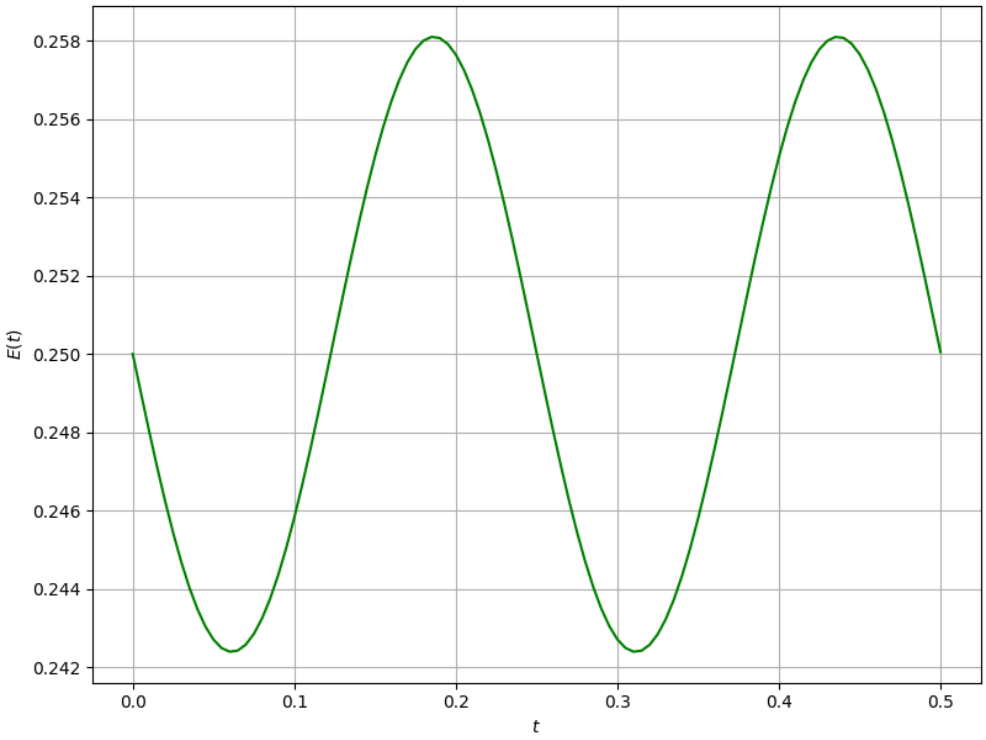

Figure 6: The energy over time, with alternating flux and $CFL = 1$.

Task 6

In this task, we examined the behavior of the numerical solution under solid wall boundary conditions with varying values of θ in the θ-scheme using **ex2no6.py**. For $\theta = 0.1$, which emphasizes the explicit part of the scheme, the numerical solution exhibited instability, with the solution jumping wildly at certain points (Figure 7). This instability occurred due to the inability of the explicit scheme to handle the steep gradients at the solid wall boundary, causing the numerical errors to amplify and leading to a breakdown in the stability of the solution. In addition, the energy of the system grew exponentially over time (Figure 8), which further highlights the instability introduced by the scheme in the presence of the solid wall boundary.

In contrast, when $\theta = 0.5$, which balances the explicit and implicit parts of the scheme, the solution remained stable and accurately captured the wave dynamics, even near the solid wall. The numerical solution closely followed the exact solution (Figure 9), and the energy fluctuated within expected bounds (Figure 10), indicating stable behavior. This stability can be attributed to the balanced nature of the $\theta = 0.5$ scheme, which managed to effectively handle the boundary reflections while maintaining the accuracy of the wave propagation.

However, when $\theta = 0.9$, which places more emphasis on the implicit part of the scheme, the solution became unstable again. The numerical solution exhibited wild jumps at certain points (Figure 11), similar to the behavior seen with $\theta = 0.1$. The energy in the system increased exponentially (Figure 12), demonstrating the breakdown of the solution due to improper handling of the solid wall boundary condition. The implicit scheme, while generally stable, caused improper reflections or artificial damping at the boundary, leading to instability.

In summary, the solid wall boundary condition presents unique challenges, particularly when using extreme values of θ in the θ-scheme. The value $\theta = 0.5$ strikes the best balance between stability and accuracy, providing stable solutions and maintaining proper energy behavior. In contrast, smaller or larger values of θ lead to instability, highlighting the importance of selecting an appropriate value for θ when dealing with solid wall boundary conditions.

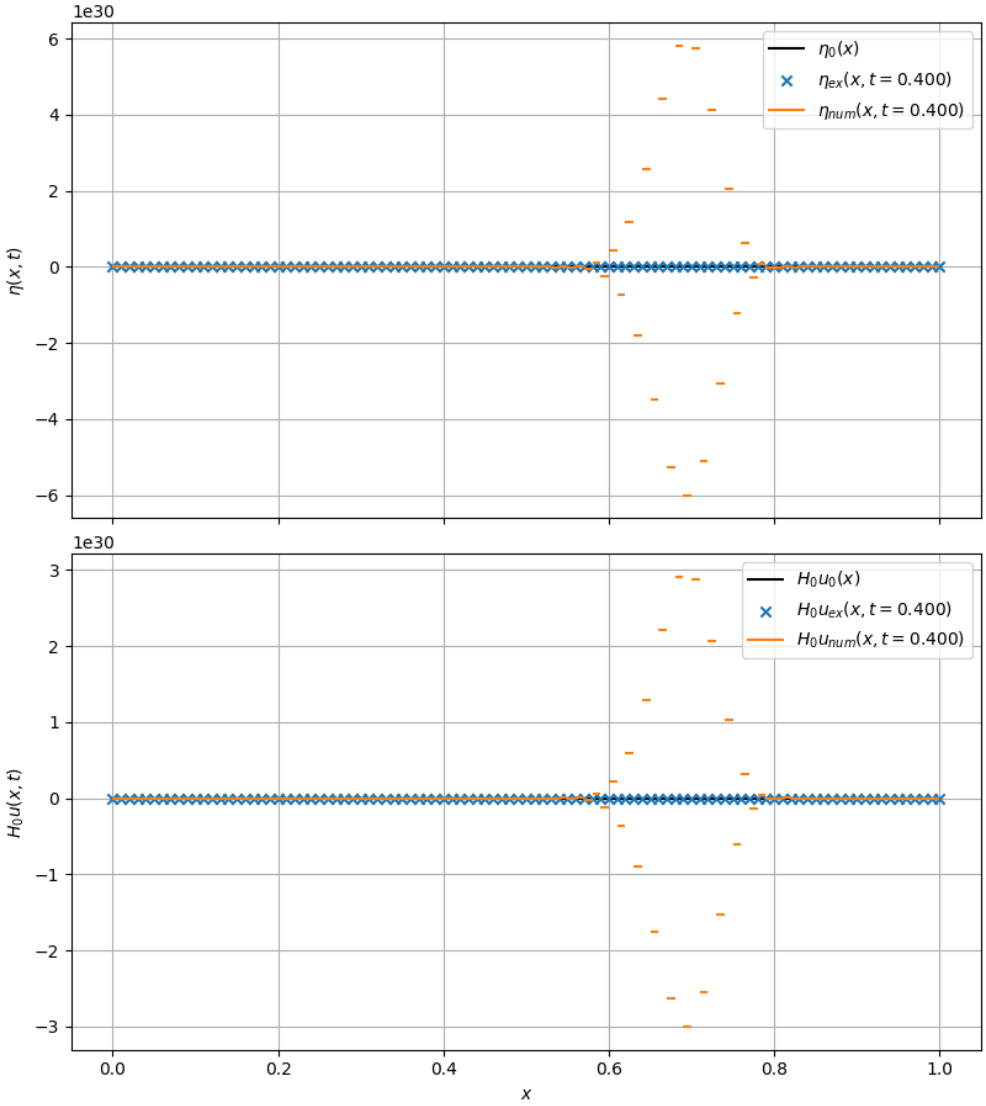

Figure 7: Numerical solution for $\theta = 0.1$ showing instability with wild jumps at some x points due to explicit dominance in the scheme.

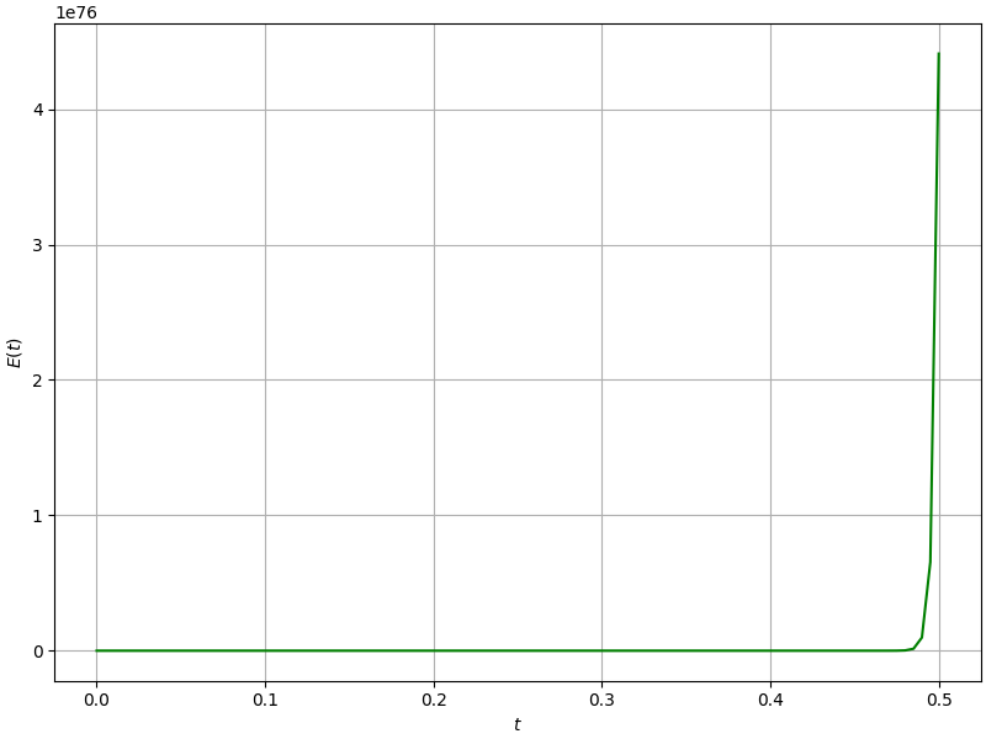

Figure 8: Energy evolution over time for $\theta = 0.1$, showing exponential growth due to instability near the solid wall boundary.

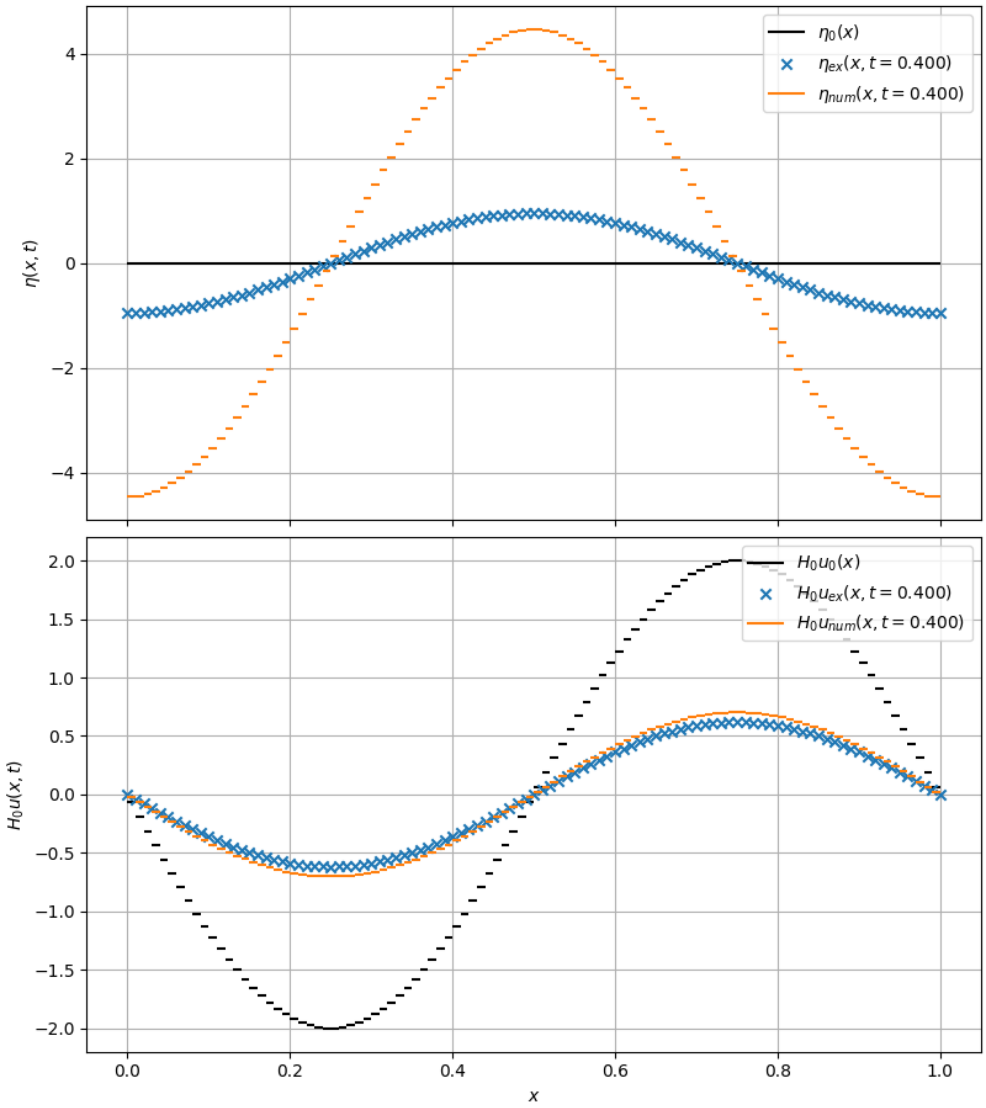

Figure 9: Numerical solution for $\theta = 0.5$ demonstrating stability and accurate reflection at the solid wall boundary.

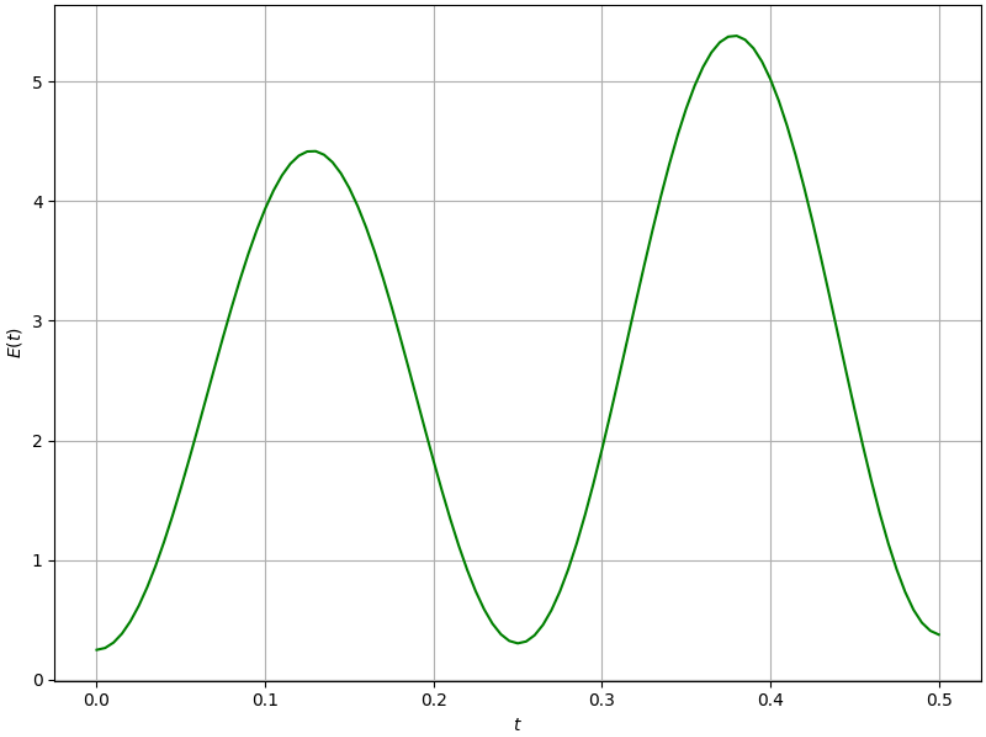

Figure 10: Energy evolution over time for $\theta = 0.5$, showing normal fluctuations, indicating stable behavior.

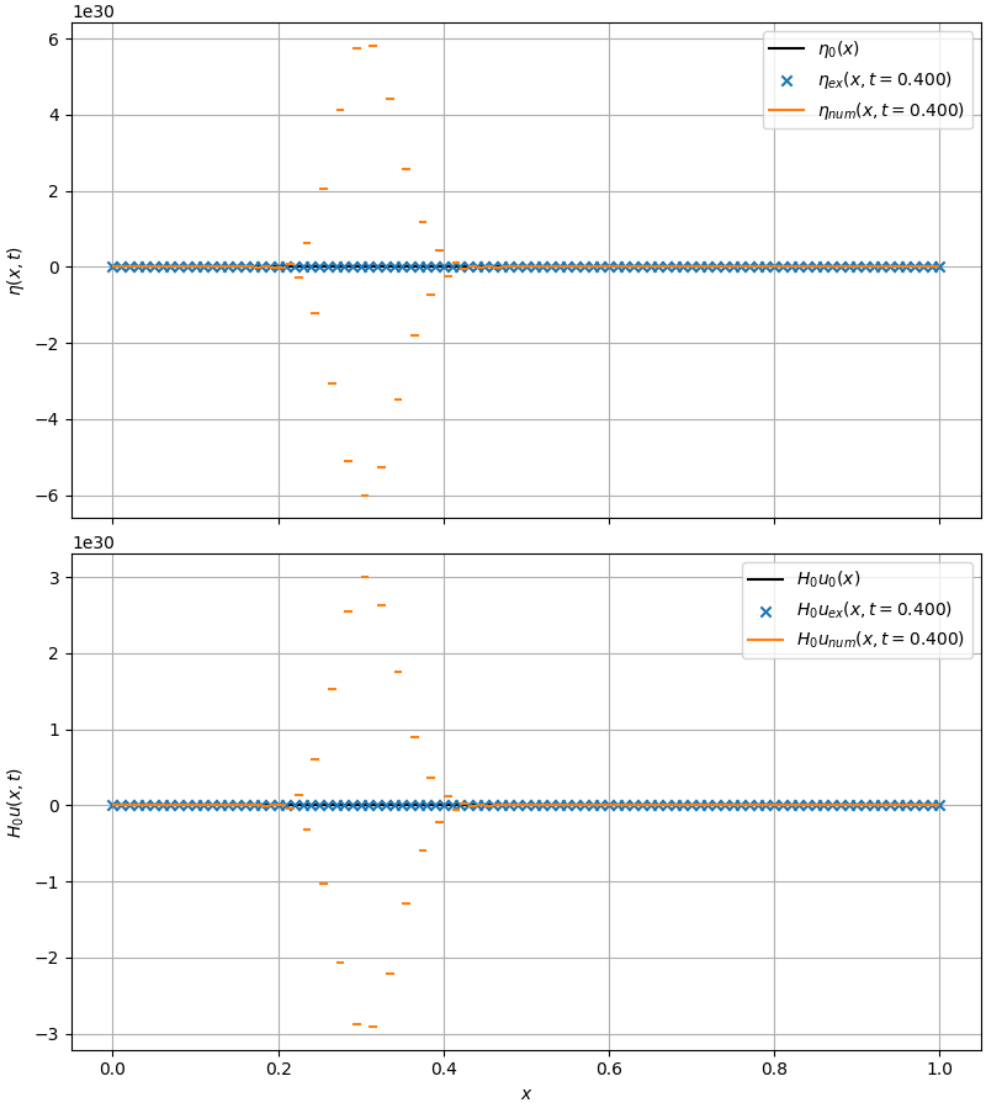

Figure 11: Numerical solution for $\theta = 0.9$ exhibiting instability with wild jumps at some x points, similar to $\theta = 0.1$.

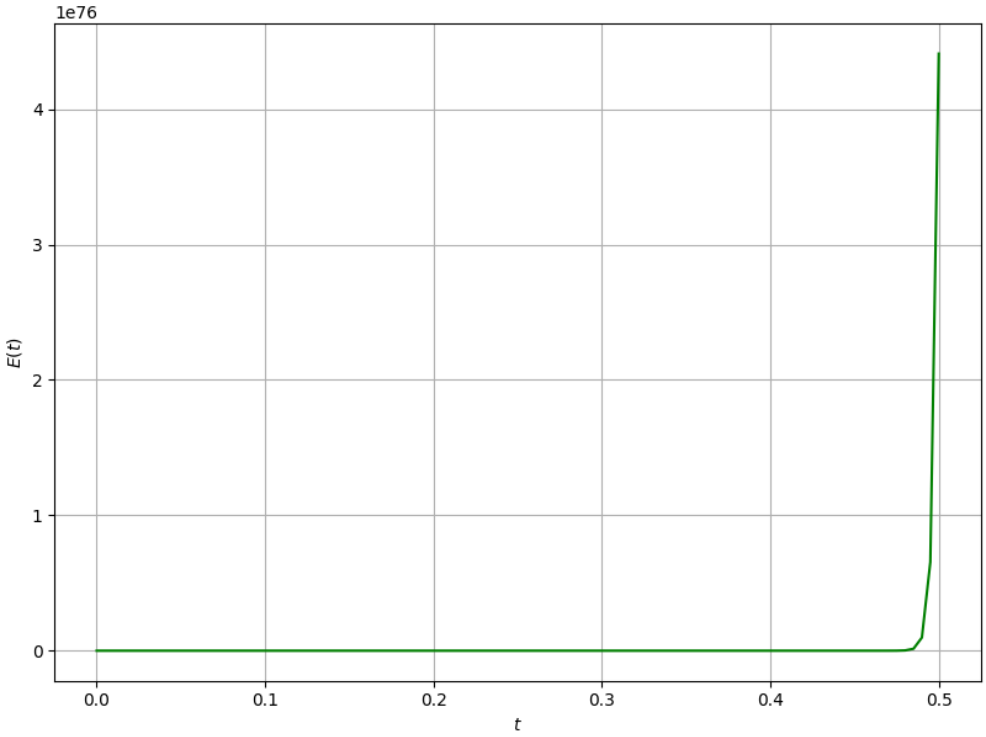

Figure 12: Energy evolution over time for $\theta = 0.9$, showing exponential growth due to instability at the solid wall boundary.

Task 8

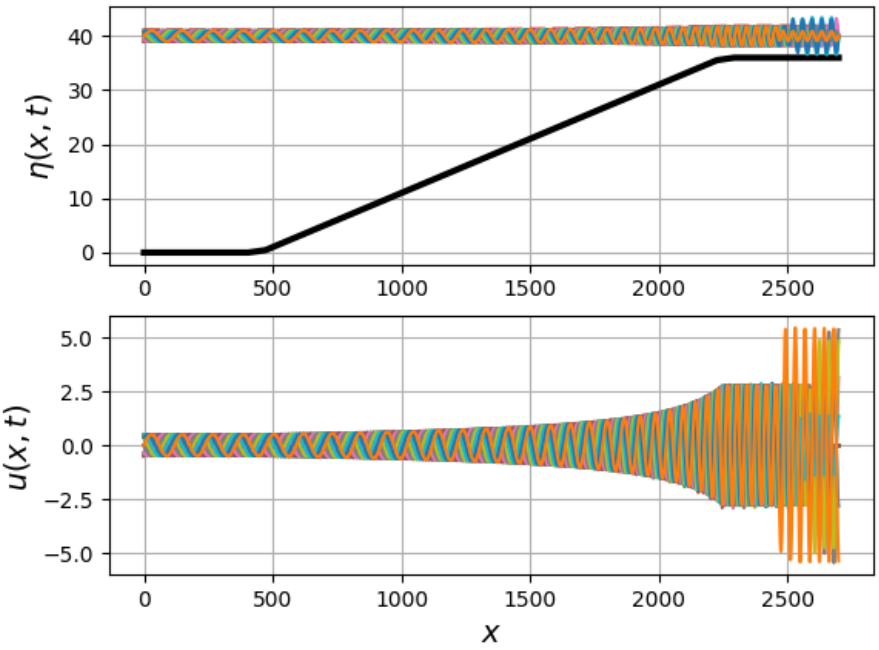

Figure 13